

Cellulose 나노크리스탈 기반의 자기치유 Polyurethane의 제조 및 물성 연구

Yang Qiao*, Qi Xu*, Shouxiang Liu*, Zhiqiang Li*, and Yanyan Wei****†

*Key Laboratory of Rubber-plastics, Ministry of Education, School of Polymer Science and Engineering,
Qingdao University of Science & Technology

**Qingdao Bifu Macromolecules Technology Co., Ltd

(2022년 11월 8일 접수, 2023년 1월 11일 수정, 2023년 2월 27일 채택)

Preparation and Properties of Cellulose Nanocrystals Based Self-healing Polyurethane

Yang Qiao*, Qi Xu*, Shouxiang Liu*, Zhiqiang Li*, and Yanyan Wei****†

*Key Laboratory of Rubber-plastics, Ministry of Education, School of Polymer Science and Engineering,
Qingdao University of Science & Technology, Qingdao, 266000, Shandong, China

**Qingdao Bifu Macromolecules Technology Co., Ltd, Qingdao, 266042, Shandong, China

(Received November 8, 2022; Revised January 11, 2023; Accepted February 27, 2023)

Abstract: First, cellulose nanocrystals were extracted from microcrystalline cellulose using the sulfuric acid hydrothermal method. Second, imine aromatic diol (Imine) was synthesized from p-hydroxybenzaldehyde and 4,4'-diaminodiphenylmethane as raw materials. Then the imine was introduced into the polyurethane, and the reversible covalent bond between the imine and the C = N group was used to endow the polyurethane with self-healing properties. Finally, cellulose nanocrystalline (CNC) was added into the self-healing polyurethane as the dispersed phase to prepare the composite. The experimental results show that with the increase of the amount of CNC, the properties of the composites increase first and then decrease, which is due to the physical cross-linking effect of proper CNC distribution in the self-healing polyurethane, it is beneficial to the mechanical properties, but the self-healing property is reduced by further increasing the content, which restricts the movement of the molecular chain. The mechanical properties of the composite with 0.049 g CNC are the best, with fracture strength reaching 20.59 MPa, approximately 1.56 times higher than that of pure self-healing polyurethane, and its elongation at break is 979%, and the self-healing efficiency reaches 84.7%, keeping an excellent level.

Keywords: self-healing polyurethane, imine bond, cellulose nanocrystal composites.

Introduction

The demand for materials has become more diverse since the 21st century. Ultraviolet radiation, mechanical and other factors are frequently affected to varying degrees of destruction in the daily use of polymer materials, while waste polymer materials are generally treated by incineration, resulting in large quantities of harmful gases. Therefore, self-healing materials were developed to extend the service life of polymer materials, achieve sustainable utilization, and achieve the goal of environmental protection. However, due to the high molecular mobil-

ity and poor mechanical properties of self-healing materials, it is critical to prepare the material with high self-healing efficiency and high mechanical strength.

There are two types of self-healing materials: intrinsic self-healing materials and external self-healing materials. This article focuses on the former. The intrinsic self-healing mechanism automatically repairs material cracks through chemical reactions involving reversible covalent bonds and non-covalent bonds. Hydrazone bond,² imine bond,³ D-A bond,⁴ borate bond,⁵ ionic bond,⁶ disulfide bond,⁷ hydrogen bond,⁸ C-NO⁹ bond, π - π stacking¹⁰ and hydrophobicity¹¹ are the most common types of intrinsic self-healing materials. The imine bond is a highly efficient reversible covalent bond, which can be dynamically converted at room temperature or under the catalysis of water without any external stimulation. In 2017, Zhang *et al.*¹² pre-

†To whom correspondence should be addressed.
yanyanwei_article@163.com, 0000-0001-8680-0057
©2023 The Polymer Society of Korea. All rights reserved.

pared a new type of polydimethylsiloxane self-healing elastomer, using imine bonds as self-healing points to introduce self-healing properties into the elastomer. The elastomer has well visible light transmittance (80%), high elongation (700%), and good room temperature self-healing ability. Surprisingly, this self-healing behavior can occur in water and even in the air at temperatures as low as -20°C . In 2020, Ding *et al.*¹³ synthesized self-healing hydrogels containing dynamic imine bonds using collagen, chitosan, and dialdehyde-terminated polyethylene glycol as raw materials. Ideally, it can help stop bleeding and heal wounds, and it can also monitor facial expressions.

Cellulose is considered the most abundant biopolymer on earth and is found mainly in plant cell walls.¹⁴ The chemical and physical properties of cellulose depend largely on its specific structure. The hydroxyl groups of β -1,4-glucan cellulose are located at C2, C3, and C6 positions. The $-\text{CH}_2\text{OH}$ side groups are arranged in trans positions relative to O5-C5 and C4-C5 bonds. Due to the supramolecular structure of cellulose, the solid-state is represented by high-order and low-order regions.¹⁵ These three hydroxyl groups have considerable reactivity, but their reactivity is also different due to different positions of connection. Therefore, on cellulose, hydroxyl groups can undergo various chemical reactions, such as oxidation reaction,¹⁶ etherification reaction,¹⁷ esterification reaction,¹⁸ and grafting reaction.¹⁹ Cellulose and cellulose, cellulose and water, cellulose internal structure can form hydrogen bonds, such structural characteristics give it many excellent properties, give cellulose in biology, medicine, papermaking, and other aspects of the application of special opportunities.

So combining cellulose with a self-healing material could be a huge success. In 2019, Khadivi *et al.*²⁰ prepared PU/CNC nanocomposites with low molecular weight. The results show that the introduction of low-content cellulose nanocrystals improves the modulus, tensile strength, and elongation at the break of the polyurethane matrix, while the properties of high-content cellulose nanocrystals decrease. In 2020, Rogerio *et al.*²¹ prepared TPU/CNC nanocomposites by melting blending method. The addition of CNC improved the thermal stability of thermoplastic polyurethane. When the treated CNC content is 5 wt%, the mechanical properties of CNC/TPU nanocomposites are better than those of pure TPU and other processed nanocomposites, and the young's modulus is increased by about 130% while maintaining significant toughness, tensile strength, and elongation at break. In 2020, Alexandre *et al.*²² reported the electrospinning of cellulose nanocrystals (CNC) enhanced polyurethane (PU) with adjustable mechanical strength. The

hardness and strength of electrospun PU/CNC films were improved to varying degrees. It was confirmed by scanning electron microscopy that PU/CNC mats with fibers aligned along the strain direction were harder and stronger than mats with non-aligned fibers. This means that their orientation is also conducive to the hardness and strength of the fiber PU/CNC nanocomposite mats.

This paper combines self-healing polyurethane and cellulose nanocrystals. First, cellulose nanocrystals are prepared by hydrothermal method. Second, a chain extender containing an imine reversible covalent bond was prepared and introduced into polyurethane to obtain a self-healing polyurethane substrate with high self-healing efficiency. Finally, cellulose nanocrystals were synthesized with self-healing polyurethane by solution blending. The mechanical properties of self-healing polyurethane materials were improved under the premise of ensuring self-healing efficiency, and the application fields of self-healing polyurethane materials were expanded. At the same time, the application of biomass materials has been broadened to help recyclable resources.

Experimental

Materials. Sulfuric acid, microcrystalline cellulose (MCC), sodium hydroxide, p-hydroxybenzaldehyde, 4,4'-diaminodiphenylmethane (MDA), polytetrahydrofuranediol-2000 (PTMEG-2000), diphenylmethane diisocyanate (HMDI), 1,4-butanediol (BDO), dibutyltin dilaurate (DBTDL), dimethyl sulfoxide (DMSO), dimethyl formamide (DMF). PTMEG-2000 purchased from Jinan guangyu chemical Co., Ltd. (China), HMDI purchased from Wanhua Chemical Group Co., Ltd. (China). The rest of the materials are purchased from Sinopharm Chemical Reagent Co., Ltd. (China).

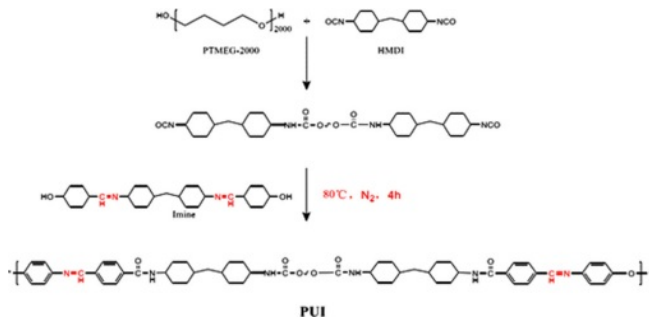
Synthesis of Cellulose Nanocrystals (CNC). A total of 4 g MCC was added into a three-mouth flask containing 64% (w v^{-1}) sulfuric acid aqueous solution and reacted at 45°C for 45 min. Finally, it was centrifuged, dialyzed, and lyophilized to obtain cellulose nanocrystalline powder, abbreviated as CNC.

Synthesis of Imine Idol (Imine). Using p-hydroxybenzaldehyde and MDA as raw material, dissolve it in anhydrous ethanol, react with nitrogen for 8 h at 80°C , and filter it several times. The yellow powder with a yield of 89% was obtained, aromatic diol, abbreviated as Imine.

Synthesis of Self-healing Polyurethane. Using PTMEG-2000 and HMDI as raw materials, the prepolymer was synthesized by inert gas reaction at 80°C for 4 h. BDO and Imine

Table 1. Raw Materials of Imine Self-healing Polyurethane with Different Contents (unit: g)

Sample	HMDI	PTMEG	BDO	IMINE
PU0	5.247	20	0.9012	0
PUI-1	5.247	20	0.7210	0.8089
PUI-2	5.247	20	0.4506	2.0223
PUI-3	5.247	20	0.1802	3.2357
PUI-4	5.247	20	0	4.0446

**Figure 1.** Schematic diagram of self-healing polyurethane with imine bond.

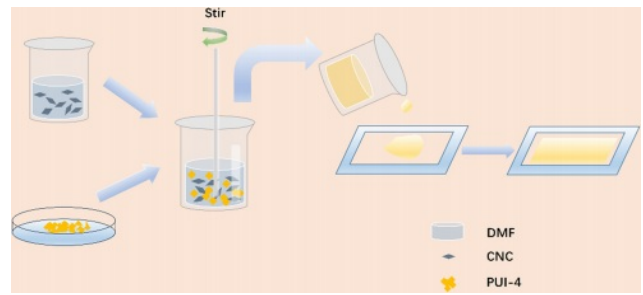
were added to the prepolymer in proportion for 4 h, and then cured and dried to obtain thermoplastic polyurethane elastomers, which were called PU0, PUI-1, PUI-2, PUI-3, and PUI-4, as shown in Table 1. The composite diagram is shown in Figure 1.

Preparation of PUI/CNC Composites. An appropriate amount of cellulose nanocrystals was placed in 24 g DMF for ultrasonic shock for 20 min, and 7 g of PUI-4 was cut into pieces, which were dissolved at 80°C and dried into films. According to the different content of CNC, they were called PUIC-1, PUIC-3, PUIC-5, PUIC-7, and PUIC-10, as shown in Table 2. Figure 2 shows the process of preparation.

Chemical Structure Characterization. The chemical structure of the sample was characterized by Fourier Infrared Transform Spectrometer (BRUKER, Germany). Cellulose nanocrystals and Imine were mixed with the appropriate amount of potassium bromide and pressed for transmission infrared test. Poly-

Table 2. Dosage Record of Self-healing Polyurethane/cellulose Nanocrystals

Sample	DMF(g)	PUI-4(g)	CNC(g)	PUI:CNC
PUIC1	24	7	0.007	1000:1
PUIC3	24	7	0.021	1000:3
PUIC5	24	7	0.035	1000:5
PUIC7	24	7	0.049	1000:7
PUIC10	24	7	0.070	1000:10

**Figure 2.** The preparation process of PUI/CNC composites.

urethane materials were tested by a reflective infrared test.

Thermal Properties Characterization. A proper amount of samples were taken for differential scanning calorimetry (NETZSCH, Germany), with the temperature range of -100~150°C, 10°C min⁻¹. Thermogravimetric tests (NETZSCH, Germany), were performed on 2 mg treated samples at a temperature range of 30~600°C and a heating rate of 20°C min⁻¹ in a nitrogen atmosphere.

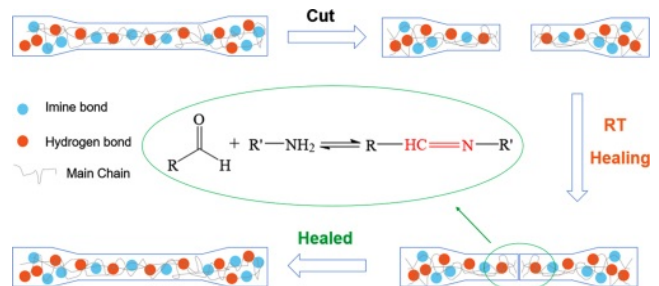
Mechanical Properties Characterization. Zwick/Roell/Z005 Electronic universal material testing machine (Zwick/Roell, Germany) was used to test the tensile properties of the cut sample at a tensile speed of 500 mm min⁻¹.

Self-healing Performance Characterization. Zwick/Roell/Z005 electronic universal material testing machine was used to test the mechanical properties of the composites after 48 h healing at room temperature after cutting. The self-healing efficiency is expressed by the following formula:

$$R\sigma = \frac{\sigma_h}{\sigma_0} \times 100\% \quad (1)$$

$$R\varepsilon = \frac{\varepsilon_h}{\varepsilon_0} \times 100\% \quad (2)$$

Where, σ_h and σ_0 are the tensile strength after healing and normal splines respectively, and ε_h and ε_0 are the elongations at the break after healing and normal splines respectively. The self-healing process of self-healing polyurethane is shown in Figure 3.

**Figure 3.** Schematic diagram of self-healing process of the self-healing polyurethane.

Results and Discussion

Chemical Structure Analysis. The infrared spectra of MCC and CNC are shown in Figure 4(a). The results show that the peak shape and peak position of the CNC infrared spectrum is consistent with those of MCC.²³ The absorption peak of CNC at 3352 cm^{-1} is wider, and it is the stretching vibration peak of -OH. For the free hydroxyl group, the absorption peak at $3650\text{--}3590\text{ cm}^{-1}$ is a medium-strength absorption band.²³ However, due to a large number of hydroxyl groups in cellulose and the strong hydrogen bonding between and within the molecules, these bands move towards the lower wavenumber, widen and increase in strength. In general, the structure of cellulose is not destroyed after the hydrothermal reaction of sulfuric acid.

Figure 4(b) shows the infrared spectrum of Imine, where the peak at 3363 cm^{-1} is the stretching vibration of O-H. The free hydroxyl stretching vibration is located at 3500 cm^{-1} . Because of the co-strangulation of the adjacent benzene ring and the easy association of hydroxyl with hydrogen, the absorption peak moves to a low wave number and broadens, overlapping with the absorption peak of $\text{-CH}_2\text{-}$. The absorption peak at

3026 cm^{-1} and 2900 cm^{-1} is C-H stretching vibration, Because the OH absorption peak moves to the low wave number, the two have a certain degree of coverage. The absorption peak at 1600 cm^{-1} is the stretching vibration of C=N .²⁴ The absorption peaks at 1502 , 1438 , and 1388 cm^{-1} are the stretching vibration of C=C in the benzene ring. In conclusion, Imine was successfully prepared.

The infrared spectra of PU0 and PUI-1~4 are shown in Figure 4(c). The absorption peak at 3348 cm^{-1} is the stretching vibration of N-H. The stretching vibration of N-H is generally located in the region of $3500\text{--}3300\text{ cm}^{-1}$, which is easy to occur association. The absorption peaks at 2940 cm^{-1} and 2860 cm^{-1} are saturated $\text{-CH}_2\text{-}$ stretching vibrations. The absorption peak at 1695 cm^{-1} is the stretching vibration of C=O . The absorption peak at 1593 cm^{-1} is a stretching vibration of C=N . Combined with the structure diagram of polyurethane, it can be seen that there are two kinds of methylene in the main chain of polyurethane, corresponding to two groups of different absorption peaks in the infrared spectrum. The stretching vibration with the absorption peak of -C-O- is located at 1107 cm^{-1} .²⁵

Enlarge the infrared spectrum at $1800\text{--}1500\text{ cm}^{-1}$, as shown in Figure 4(d). With the addition of Imine, the C=N- absorp-

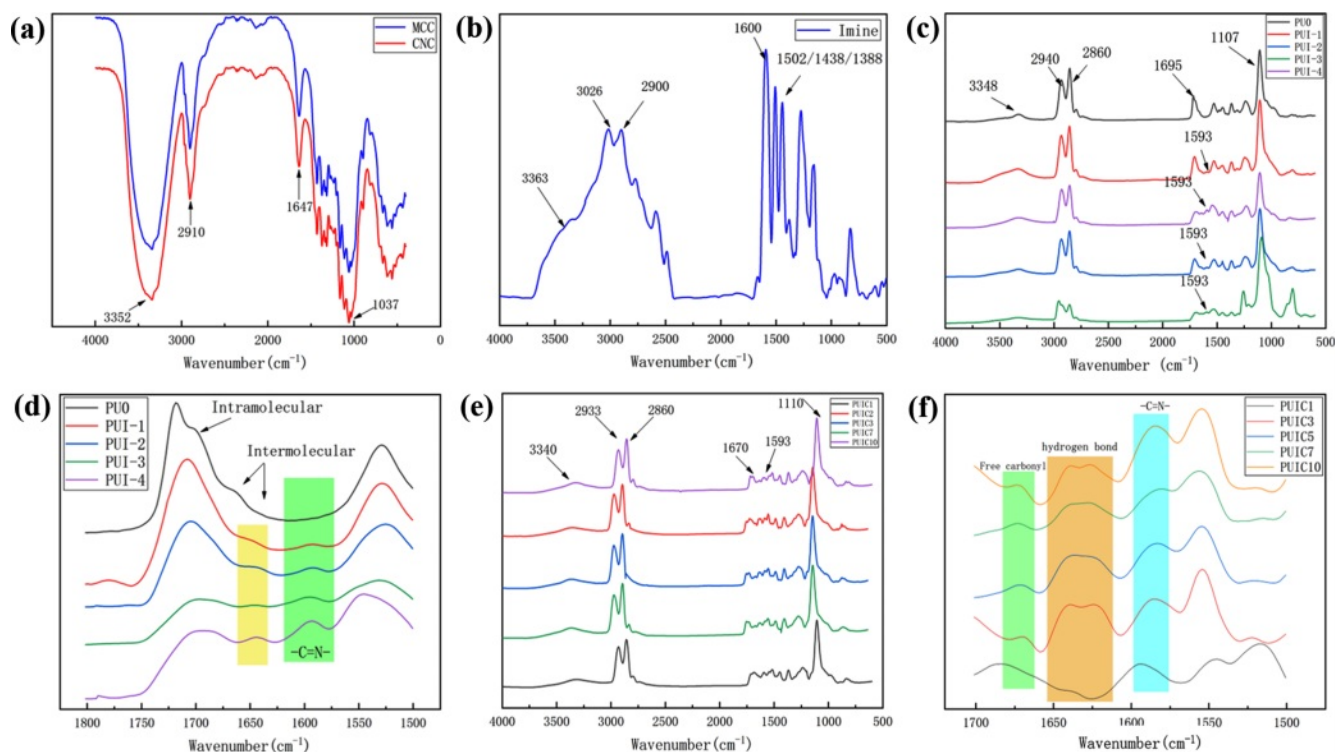


Figure 4. Infrared spectra of (a) CNC; (b) Imine; (c) PU0 and PUI-1~4; (d) Local magnified infrared spectra of PU0 and PUI-1~4; (e) PUIC 1~10; (f) Partial infrared magnification of PUIC1~10.

tion peak at 1593 cm^{-1} appeared and gradually increased, indicating that Imine was successfully bonded to polyurethane. In the local magnification spectra of PUI-1~4, the absorption peaks at about 1695 cm^{-1} and 1641 cm^{-1} are the absorption peaks of the carbonyl group, with the former representing the free carbonyl group and the latter representing the carbonyl group forming a hydrogen bond. It is also easy to see in the figure that the C=N bond has only a single peak, which indicates that the C=N bond does not form hydrogen bonds with N-H in polyurethane. Due to the high steric hindrance of the four benzene rings in Imine, the intramolecular distance of polyurethane increases, and no intramolecular hydrogen bond is generated. Therefore, the carbonyl group of polyurethane containing Imine bond can only be divided into two different absorption peaks. In general, the C=N bond in Imine cannot form a hydrogen bond with the N-H bond, and all the hydrogen bonds in the material come from the intermolecular hydrogen bond of polyurethane.

It can be seen from Figure 4(e) that the infrared spectrum of PUIC is essentially consistent with that of PUI. The infrared spectrum of $1700\sim 1500\text{ cm}^{-1}$ was amplified, and Figure 4(f) was obtained. It can be known that the infrared local magnification of PUIC1 is consistent with PUI-4. The free carbonyl peak is located at 1695 cm^{-1} , and an absorption peak is separated at 1641 cm^{-1} . The absorption peak of this carbonyl group indicates that the carbonyl group and amino group produce hydrogen bond interaction between polyurethane molecules. However, the dosage of cellulose nanocrystals in PUIC1 is only 0.1, which is not enough to form hydrogen bonds with polyurethane. PUIC3~10 showed a free carbonyl absorption peak at 1670 cm^{-1} , and two carbonyl peaks were separated from 1640 cm^{-1} and 1625 cm^{-1} . The latter two carbonyl peaks were derived from the hydrogen bonding between the carbonyl group and amino group in polyurethane and the hydrogen bonding between the carbonyl group and cellulose nanocrystalline in polyurethane. In conclusion, the addition of cellulose nanocrystals will increase the type and strength of hydrogen bonds in self-healing polyurethane materials.

Thermal Performance Analysis. As can be seen from Figure 5(a), both PU0 and PUI-1~4 have only one glass transition temperature (T_g). Because the self-healing polyurethane prepared in this paper is thermoplastic polyurethane without a crosslinking agent, the content of the hard segment is low. Therefore, it is difficult to see the second T_g in the DSC curve. The T_g of all tested substances is below room temperature (25°C), so they are in a state of high elasticity at room temperature, which is a kind of elastic body. The T_g of PUI-1~4 increases

with the increase of imine content, which is due to the increase of the content of imine bond, the increase of the number of benzene rings contained in the molecular chain, and the increase of the steric resistance between the molecular chains, thus affecting the T_g of the material.

PUI/CNC composites have only one T_g , which is below room temperature, as shown in Figure 5(b). After the addition of cellulose nanocrystals, the properties of the composites are substantially unchanged, and they are all elastomers. It can be seen that compared with PUIC1~10, the T_g of polyurethane matrix PUI-4 decreases slightly except for PUIC1,²⁶ its trend is: the T_g of self-healing polyurethane/cellulose nanocrystals composites increased with the increase of cellulose nanocrystals content, but the change was not obvious. Cellulose nanocrystals contain a large number of hydroxyl groups and their intermolecular and intramolecular hydrogen bonds are very strong. The polyurethane prepared in this paper has a low molecular weight. When the number of CNC additions is small, the hydrogen bond binding force is weak. The Coulomb force of the sulfonic acid group in the CNC harms the crystallization of the material, thereby reducing the T_g . When the CNC content gradually increased, it produced stronger hydrogen bonding with the polyurethane molecular chain, and the crystallization ability was enhanced, so the glass transition temperature increased. However, due to the small number of cellulose nanocrystals, the glass transition temperature only changed slightly.

It can be seen from Figure 5(c) that both PU0 and PUI-1~4 have two stages of thermal weightlessness. The 5% Td (weight loss 5% temperature) of PU0 is 273°C , the weight loss range is $224\sim 248^\circ\text{C}$ and $348\sim 489^\circ\text{C}$ respectively, and the residual amount is 1.33%. The first weight loss range of PU0 is caused by the C-O bond, C-N bond, and C=O bond in the polyurethane main chain, which contain electron-sucking atoms and break at a lower temperature than the C-C bond. When the temperature reached 408°C , the C-C bond in the polyurethane main chain began to fracture and decomposed completely at 489°C . The thermogravimetric curves of PUI-1 to PUI-4 are mostly the same, and the two weight loss ranges are $321\sim 362^\circ\text{C}$ and $362\sim 500^\circ\text{C}$ respectively. Compared with PU0, the weight loss temperature of PUI-1~4 is improved to a certain extent. This change is caused by the different chain extenders used in the reaction process. The main chain of 1, 4-butandiol is a soft carbon chain with a lower breaking temperature, while the main chain of imine aromatic diol has four rigid benzene rings with a higher breaking temperature. Therefore, PUI-1~4 has higher thermal stability than PU0. However, the T_g curves of PUI-1~4

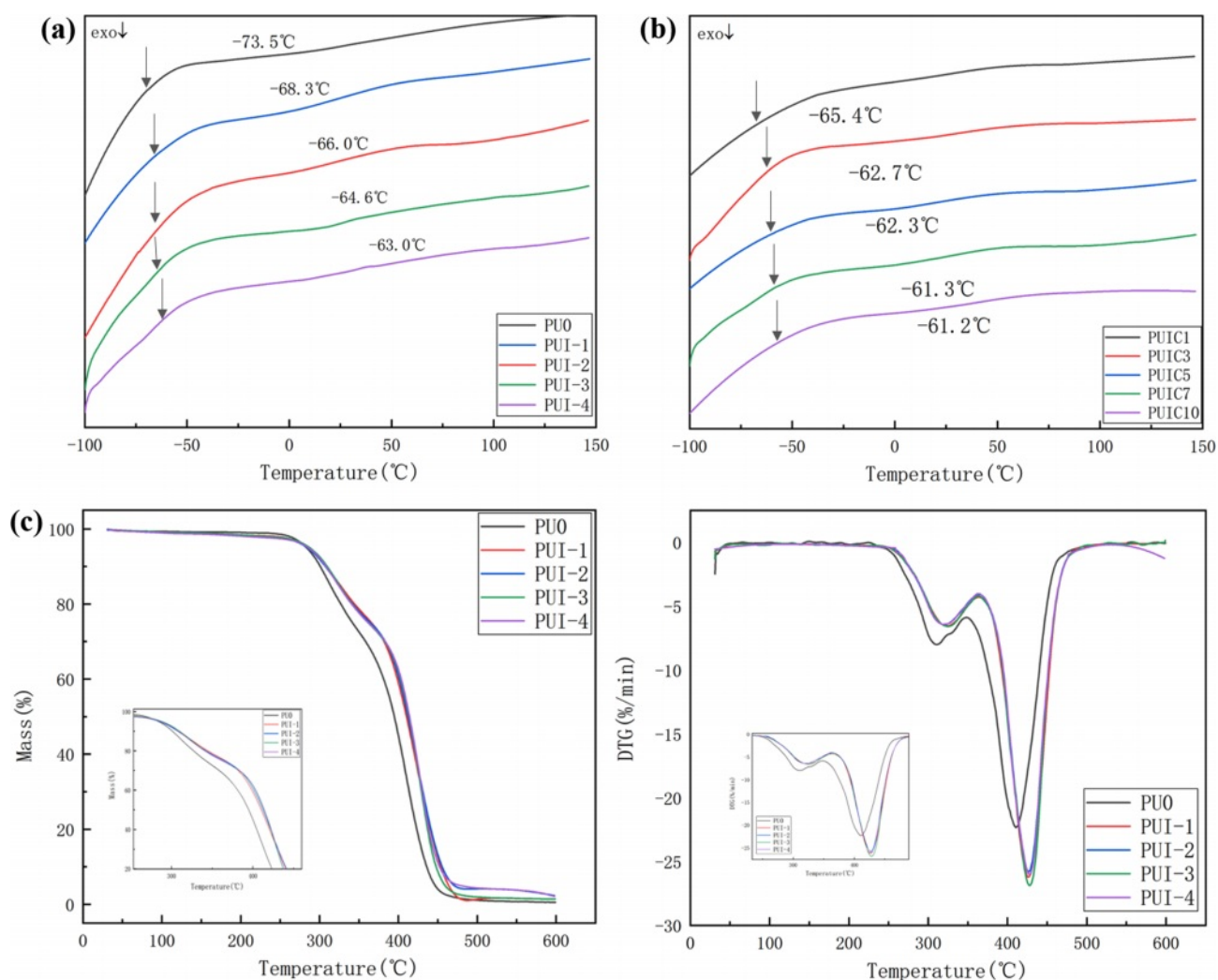


Figure 5. (a) DSC curves of PU0 and PUI-1~4; (b) DSC curve of PUIC1~10; (c) TGA and DTG curves of PU0 and PUI-1~4.

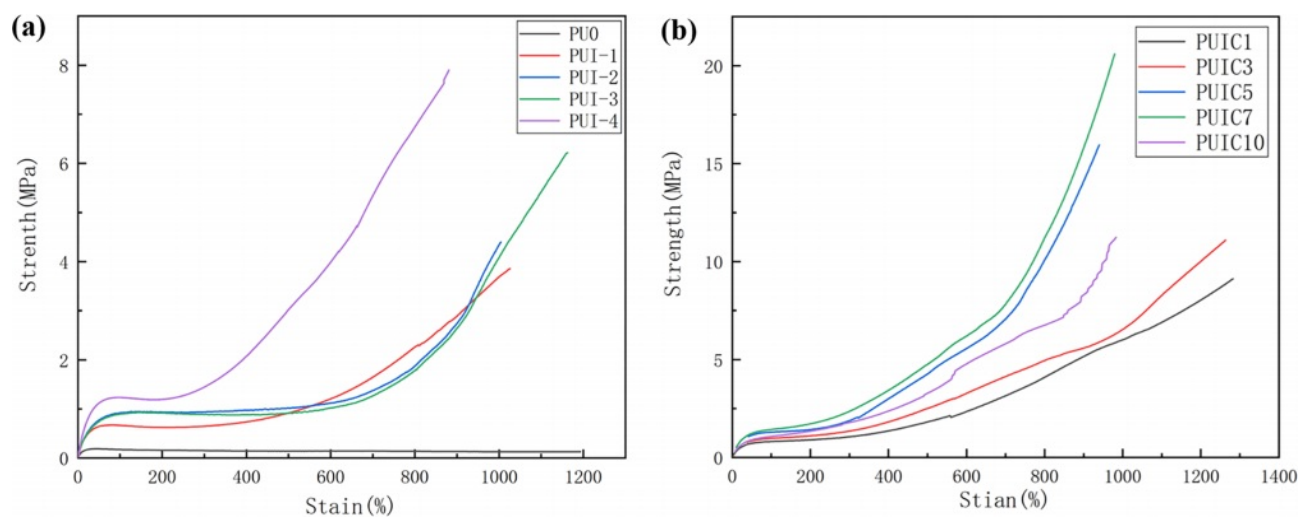


Figure 6. Mechanical property curves: (a) PU0 and PUI-1~4; (b) PUIC1~10.

Table 3. Mechanical Properties Record of Self-healing Polyurethane

Sample	PU0	PUI-1	PUI-2	PUI-3	PUI-4
σ_0 (MPa)	0.13	3.86	4.39	6.23	8.03
ε_0 (%)	1193	1036	1004	1123	883

almost overlap with those of TGA, indicating that the effect of imine aromatic diol chain extender on the thermal stability of self-healing polyurethane is limited.

Mechanical Property Analysis. The mechanical properties of the self-healing polyurethane material are shown in Figure 6(a) and Table 3. In the self-healing polyurethane material based on imine bond, when the content of imine diol changes from 0 to 10, the fracture strength of the material increases significantly from 0.13 to 3.86 MPa, while the elongation at break decreases slightly. The imine bond is bonded to the polyurethane main chain, which gives the self-healing polyurethane a certain rigidity. Moreover, because the material is a thermoplastic elastomer, the content of the hard segment is low, the molecular chain is crosslinked only by a weak hydrogen bond, and the rigid chain segment is crosslinked without the crosslinking agent, so the change of elongation at break is small. To sum up, the breaking strength is significantly increased, while the elongation at break is slightly decreased. With the imine content changing from 10% to 50%, the fracture strength and elongation at the break of self-healing polyurethane increased with the increase of imine content, but the overall trend was reduced, but it remained at a good level. PUI-4 has the best mechanical properties, and its mechanical strength can reach 8.03 MPa without the action of crosslinking agent.

As shown in Figure 6(b) and Table 4, when the dosage of cellulose nanocrystals changes from 0 to 0.1 parts, the fracture strength changes from 8.03 to 9.12 MPa, increasing by 1.04 MPa. Elongation at break changed from 883 to 1283%, an increase of 400%. Both breaking strength and elongation at break increased significantly. Compared with PUI-4, PUIC1 contains cellulose nanocrystals with active hydroxyl groups. Cellulose nanocrystals are distributed in the self-healing polyurethane, and the active group hydroxyl will produce a hydrogen bond with the C=O in the main chain of the polyurethane, playing a role in physical cross-linking. Under the action of

Table 4. The Mechanical Performance Record of PUIC1~10

Sample	PUI-4	PUIC1	PUIC3	PUIC5	PUIC7	PUIC10
σ_0 (MPa)	8.03	9.12	11.08	15.94	20.59	11.23
ε_0 (%)	883	1283	1269	948	979	983

such physical crosslinking, the molecular weight of polyurethane molecular chains is increased by hydrogen bonding, so the fracture strength and elongation at the break of the material will be improved to varying degrees at the same time. The breaking strength of PUIC1~10 increased first and then decreased with the increase of cellulose nanocrystals, while the elongation at break decreased continuously. PUIC7 has the highest fracture strength of 20.59 MPa. The mechanical properties of PUIC10 decreased because of the decreased dispersion of cellulose nanocrystals in the self-healing polyurethane and aggregation in the matrix. The intermolecular hydrogen bond of cellulose nanocrystals itself was too large to bond the polyurethane closely.

Self-healing Performance Analysis. The self-healing polyurethane film is cut into dumbbell-shaped samples, cut off completely from the middle, and then the section is aligned and fitted. The self-healing samples were obtained after 48 h at room temperature and were named PU0-SH, PUI-1-SH, PUI-2-SH, PUI-3-SH, and PUI-4-SH respectively. The mechanical properties of these samples are shown in Figure 7(a). According to formulas (1) and (2), the self-healing efficiency of materials is calculated (as shown in Figure 7(b) and Table 5). $R\sigma$ of PUI-1~4 is 61.7, 72.9, 85.7, and 96.4%, and $R\varepsilon$ is 86.5, 86.0, 85.9, and 90.3%, respectively. According to the variation of data, it can be concluded that the self-healing efficiency of the material increases with the increase of the concentration of polyurethane imine bond. General polyurethanes have self-healing properties due to the dissociation and formation of hydrogen bonds at high temperatures, but poor self-healing properties at room temperature. Therefore, in the self-healing polyurethane prepared in this chapter, the imine bond plays a leading role in the self-healing process. In summary, the imine bond is a reversible covalent bond with high self-healing efficiency, which has a significant effect on polyurethane. In the dosage range of 10~50%, with the increase of concentration, the self-healing performance of the self-healing polyurethane material also increases, among which PUI-4 has the best self-healing per-

Table 5. The Mechanical Properties and Self-healing Efficiency Records of PU0 and PUI-1~4

Sample	σ_0	ε_0	σ_{SH}	ε_{SH}	$R\sigma$ (%)	$R\varepsilon$ (%)
PU0-SH	0.13	1193	—	—	—	—
PUI-1-SH	3.86	1026	2.38	888	61.7	86.5
PUI-2-SH	4.39	1004	3.20	864	72.9	86.0
PUI-3-SH	6.23	1163	5.34	999	85.7	85.9
PUI-4-SH	8.03	883	7.74	796	96.4	90.3

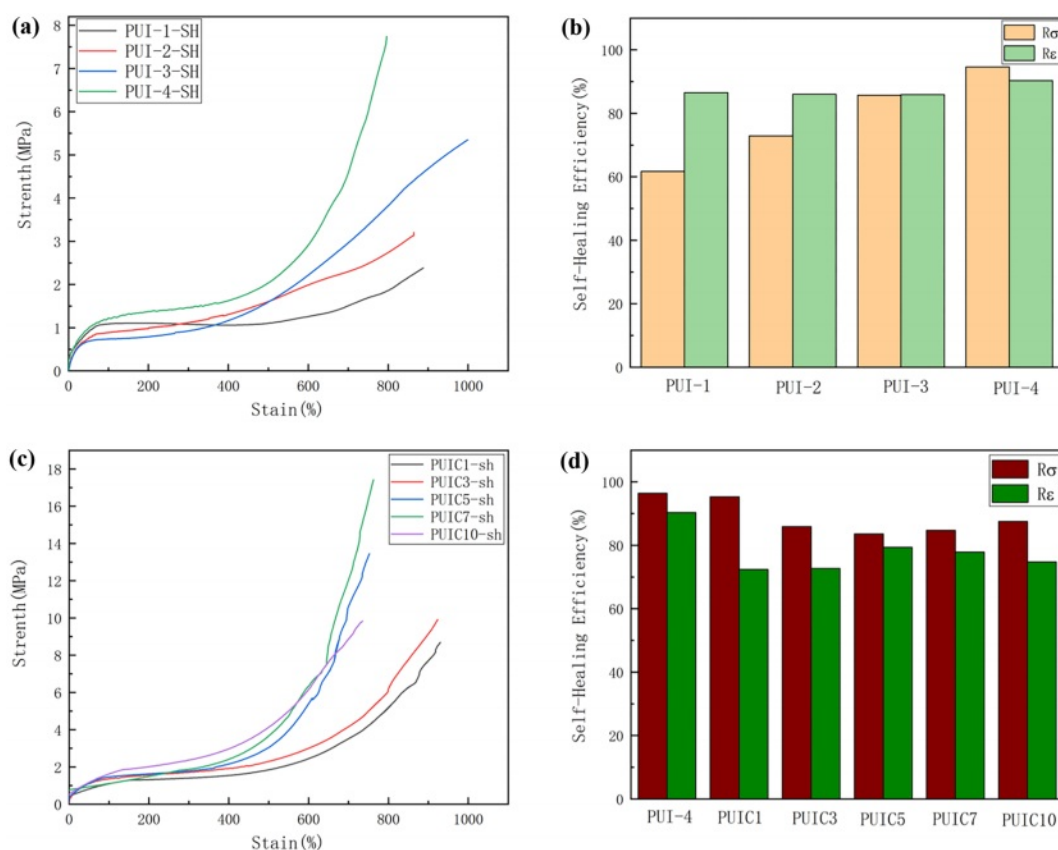


Figure 7. (a) Mechanical properties curves of PU0 and PUI-1~4 after self-healing; (b) variation trend of self-healing efficiency of self-healing polyurethane; (c) mechanical property curve of PUIC1~10 after self-healing; (d) variation trend of self-healing efficiency of PUI/CNC.

formance. Therefore, PUI-4 is suitable for subsequent experiments.

The self-healing polyurethane/cellulose nanocrystalline composite films are called PUIC1-sh, PUIC3-sh, PUIC5-sh, PUIC7-sh, and PUIC10-sh. As can be seen from the Figure 7(c) and Figure 7(d), the breaking strength of PUIC1~10-sh is 8.69, 9.92, 13.34, 17.43, and 9.83 MPa, and the elongation at break is 930, 923, 753, 763, and 735%, respectively. The fracture strength and elongation at the break of PUIC 1~10 specimens are reduced to different degrees. Specific comparisons are shown in Table 6.

The $R\sigma$ of PUI-4 and PUIC 1~10 were 96.4, 95.3, 89.5, 83.6, 84.7, and 87.5%, respectively. The self-healing efficiency of the PUIC-sh series is slightly lower than that of PUI-4-SH. With the increase in the number of cellulose nanocrystals, the hydrogen bonding effect is enhanced, and the flexibility of the main chain of the molecule becomes worse, affecting the movement of the chain segment, so the $R\epsilon$ decreases significantly. In conclusion, the self-healing efficiency of the self-healing polyurethane with cellulose nanocrystals added is lower than that

Table 6. Mechanical Properties and Self-healing Efficiency Record of PUIC1~10

Sample	σ_0	ϵ_0	σ_{SH}	ϵ_{SH}	R_σ (%)	R_ϵ (%)
PUI-4-SH	8.03	883	7.74	796	96.4	90.3
PUIC1-sh	9.12	1283	8.69	930	95.3	72.4
PUIC3-sh	11.08	1269	9.92	923	89.5	72.7
PUIC5-sh	15.94	948	13.34	753	83.6	79.4
PUIC7-sh	20.59	979	17.43	763	84.7	77.9
PUIC10-sh	11.23	983	9.83	735	87.5	74.8

of the self-healing polyurethane matrix, and with the increase of the cellulose nanocrystals added, the self-healing efficiency also decreases, but the overall is still in an excellent range, and the self-healing conditions are very mild.

Strengthening Mechanism of PUI/CNC Composites. To study the strengthening mechanism of the composites, the carbonyl absorption peaks of PUI-4 and PUIC1~10 were fitted with Gaussian.²⁷ The free carbonyl group in polyurethane, the carbonyl group²⁸ that produces hydrogen bonding with the

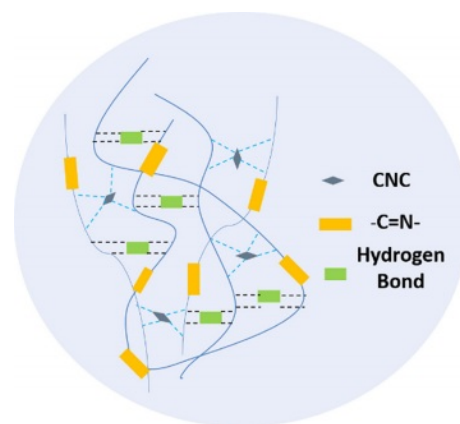
Table 7. Hydrogen Bond Fitting Results of PUIC1~10

Sample	Peaks	Wavenumbers (cm ⁻¹)	Proportion (%)
PUI-4	I	1695	18.68
	II	1647	81.32
PUIC1	I	1695	16.37
	II	1641	83.63
PUIC3	I	1670	20.00
	II	1640	10.18
	III	1625	69.81
PUIC5	I	1670	13.97
	II	1640	56.06
	III	1625	29.97
PUIC7	I	1670	10.64
	II	1640	34.22
	III	1625	55.14
PUIC10	I	1670	24.00
	II	1640	55.86
	III	1625	20.14

amino group in polyurethane, and the carbonyl group that produces hydrogen bonding between polyurethane and cellulose nanocrystals are expressed as I, II, and III. The percentages of different hydrogen bond types were obtained as shown in Table 7.

It can be seen from Table 7 that in addition to the increase in the percentage of free carbonyl in PUIC3, the trend of the whole group of samples showed a trend of first increasing and then decreasing. The addition of cellulose nanocrystals increased the hydrogen bonding of polyurethane, and the percentage of free carbonyl groups decreased from 18.68% of PUI-4 to 10.64% of PUIC7, and then increased to 24% of PUIC10.

Cellulose nanocrystals act as physical crosslinking points in self-healing polyurethanes. Strong hydrogen bonding reduces the distance between polyurethane molecules, and the crosslinking points attract many polyurethane molecular chains to form a physical crosslinking network, which increases the molecular weight of the composites at room temperature, as shown in Figure 8. The formation of a physical crosslinking network increases the elasticity and strength of the material. However, the increase of the carbonyl group in PUIC10 is due to the inhomogeneous dispersion of cellulose nanocrystals in polyurethane. The hydrogen bond between cellulose nanocrystals exceeds that between cellulose nanocrystals and polyurethane, and the carbonyl group cannot form a hydrogen bond

**Figure 8.** Strengthening mechanism.

with more N-H bonds.

In general, the addition of cellulose nanocrystals increases the hydrogen bonding in polyurethane, which affects other properties.

Conclusions

In this paper, a series of self-healing polyurethanes were prepared based on dynamic imine bonds. The introduction of imine bonds endows polyurethane materials with good mechanical properties, thermal properties, and self-healing properties. Then a series of PUI/CNC composites were prepared by selecting PUI-4, which has the best self-healing and mechanical properties, as the matrix of composites and using CNC as the dispersed phase. CNC acts as a physical crosslinking point in self-healing polyurethanes, which improves the performance of self-healing polyurethanes by bonding the polyurethane molecular chains together through hydrogen bonding. Polyurethane with 0.7% cellulose nanocrystals has the highest mechanical strength, tensile strength of 20.59 MPa, and elongation at a break of 979%. In addition to high mechanical properties, it also has considerable self-healing efficiency, up to 84.7%. Compared with 96% of polyurethane matrix, it has a slight decrease, but it still keeps a good overall level.

Acknowledgment: We gratefully acknowledge financial support from the Shandong province science and technology small and medium-sized enterprise innovation capacity improvement project: 2021TSGC1198.

Conflict of Interest: The authors declare that there is no conflict of interest.

References

1. Li, Y.; Yang, Z.; Zhao, X.; Zhang, J.; Ding, L.; Pan, L.; Lin, C.; Zheng, X. Practicable Self-healing Polyurethane Binder for Energetic Composites Combining Thermo-reversible DA Action and Shape-memory Effect. *Polym. Adv. Technol.* **2021**, *32*, 4223-4232.
2. Wang, X.; Wei, Y.; Chen, D.; Bai, Y. Synthesis and Properties of Room-Temperature Self-Healing Polyurethane Elastomers. *J. Macromol. Sci., Part A* **2017**, *54*, 956-966.
3. Dai, X.; Du, Y.; Wang, Y.; Liu, Y.; Xu, N.; Li, Y.; Shan, D.; Xu, B. B.; Kong, J. Stretchable Self-Healing Polymeric Networks with Recyclability and Dual Responsiveness. *ACS Appl. Polym. Mater.* **2020**, *2*, 1065-1072.
4. Guo, M.; Chen, L.; Fang, T.; Wang, R.; Nuraje, N.; Brodelius, P. E. Synthesis, Properties and Applications of Self-repairing Carbohydrates as Smart Materials via Thermally Reversible DA Bonds. *Polym. Adv. Technol.* **2021**, *32*, 1026-1037.
5. Cromwell, O. R.; Chung, J.; Guan, Z. Malleable and Self-Healing Covalent Polymer Networks through Tunable Dynamic Boronic Ester Bonds. *J. Am. Chem. Soc.* **2015**, *137*, 6492-6495.
6. Zhang, L.; Xiong, H.; Wu, Q.; Peng, Y.; Zhu, Y.; Wang, H.; Yang, Y.; Liu, X.; Huang, G.; Wu, J. Constructing Hydrophobic Protection for Ionic Interactions toward Water, Acid, and Base-Resistant Self-Healing Elastomers and Electronic Devices. *Sci. China Mater.* **2021**, *64*, 1780-1790.
7. Li, Z.-J.; Zhong, J.; Liu, M.-C.; Rong, J.-C.; Yang, K.; Zhou, J.-Y.; Shen, L.; Gao, F.; He, H.-F. Investigation on Self-Healing Property of Epoxy Resins Based on Disulfide Dynamic Links. *Chin. J. Polym. Sci.* **2020**, *38*, 932-940.
8. Nie, J.; Huang, J.; Fan, J.; Cao, L.; Xu, C.; Chen, Y. Strengthened, Self-Healing, and Conductive ENR-Based Composites Based on Multiple Hydrogen Bonding Interactions. *ACS Sustainable Chem. Eng.* **2020**, *8*, 13724-13733.
9. Zuo, X.; Chang, K.; Zhao, J.; Xie, Z.; Tang, H.; Li, B.; Chang, Z. Bubble-Template-Assisted Synthesis of Hollow Fullerene-like MoS₂ Nanocages as a Lithium Ion Battery Anode Material. *J. Mater. Chem. A* **2016**, *4*, 51-58.
10. Feula, A.; Pethybridge, A.; Giannakopoulos, I.; Tang, X.; Chippindale, A.; Siviour, C. R.; Buckley, C. P.; Hamley, I. W.; Hayes, W. A Thermoreversible Supramolecular Polyurethane with Excellent Healing Ability at 45 °C. *Macromolecules* **2015**, *48*, 6132-6141.
11. Davydovich, D.; Urban, M. W. Water Accelerated Self-Healing of Hydrophobic Copolymers. *Nat Commun.* **2020**, *11*, 5743.
12. Zhang, B.; Zhang, P.; Zhang, H.; Yan, C.; Zheng, Z.; Wu, B.; Yu, Y. A Transparent, Highly Stretchable, Autonomous Self-Healing Poly(Dimethyl Siloxane) Elastomer. *Macromol. Rapid Commun.* **2017**, *38*, 1700110.
13. Ding, C.; Tian, M.; Feng, R.; Dang, Y.; Zhang, M. Novel Self-Healing Hydrogel with Injectable, PH-Responsive, Strain-Sensitive, Promoting Wound-Healing, and Hemostatic Properties Based on Collagen and Chitosan. *ACS Biomater. Sci. Eng.* **2020**, *6*, 3855-3867.
14. Ahmed-Haras, M. R.; Kao, N.; Ward, L. Single-Step Heterogeneous Catalysis Production of Highly Monodisperse Spherical Nanocrystalline Cellulose. *Int. J. Biol. Macromol.* **2020**, *154*, 246-255.
15. Klemm, D.; Heublein, B.; Fink, H.-P.; Bohn, A. Cellulose: Fascinating Biopolymer and Sustainable Raw Material. *Angew. Chem. Int. Ed.* **2005**, *44*, 3358-3393.
16. Mahrous, F.; Koshani, R.; Tavakolian, M.; Conley, K.; van de Ven, T. G. M. Formation of Hairy Cellulose Nanocrystals by Cryogrinding. *Cellulose* **2021**, *28*, 8387-8403.
17. Gu, H.; Gao, X.; Zhang, H.; Chen, K.; Peng, L. Fabrication and Characterization of Cellulose Nanoparticles from Maize Stalk Pith via Ultrasonic-Mediated Cationic Etherification. *Ultrasonics Sonochemistry* **2020**, *66*, 104932.
18. Wang, X.; Wang, N.; Xu, B.; Wang, Y.; Lang, J.; Lu, J.; Chen, G.; Zhang, H. Comparative Study on Different Modified Preparation Methods of Cellulose Nanocrystalline. *Polymers* **2021**, *13*, 3417.
19. Roy, D.; Semsarilar, M.; Guthrie, J. T.; Perrier, S. Cellulose Modification by Polymer Grafting: A Review. *Chem. Soc. Rev.* **2009**, *38*, 2046-2064.
20. Khadivi, P.; Salami-Kalajahi, M.; Roghani-Mamaqani, H.; Lotfi Mayan Sofla, R. Fabrication of Microphase-Separated Polyurethane/Cellulose Nanocrystal Nanocomposites with Irregular Mechanical and Shape Memory Properties. *Appl. Phys. A* **2019**, *125*, 779.
21. Prataiviera, R.; Pollet, E.; Bretas, R. E. S.; Avérous, L.; Almeida Lucas, A. Melt Processing of Nanocomposites of Cellulose Nanocrystals with Biobased Thermoplastic Polyurethane. *J. Appl. Polym. Sci.* **2021**, *138*, 50343.
22. Redondo, A.; Jang, D.; Korley, L. T. J.; Gunkel, I.; Steiner, U. Electrospinning of Cellulose Nanocrystal-Reinforced Polyurethane Fibrous Mats. *Polymers* **2020**, *12*, 1021.
23. Sheikhy, S.; Safekordi, A. A.; Ghorbani, M.; Adibkia, K.; Hamishehkar, H. Synthesis of Novel Superdisintegrants for Pharmaceutical Tableting Based on Functionalized Nanocellulose Hydrogels. *Int. J. Biol. Macromol.* **2021**, *167*, 667-675.
24. Wang, P.; Yang, L.; Dai, B.; Yang, Z.; Guo, S.; Gao, G.; Xu, L.; Sun, M.; Yao, K.; Zhu, J. A Self-Healing Transparent Polydimethylsiloxane Elastomer Based on Imine Bonds. *Eur. Polym. J.* **2020**, *123*, 109382.
25. Hu, J.; Mo, R.; Sheng, X.; Zhang, X. A Self-Healing Polyurethane Elastomer with Excellent Mechanical Properties Based on Phase-Locked Dynamic Imine Bonds. *Polym. Chem.* **2020**, *11*, 2585-2594.
26. Zhu, Y.; Hu, J. L.; Yeung, K. W.; Liu, Y. Q.; Liem, H. M. Influence of Ionic Groups on the Crystallization and Melting Behavior of Segmented Polyurethane Ionomers. *J. Appl. Polym. Sci.* **2006**, *100*, 4603-4613.
27. Yu, J.; Wang, K.; Fan, C.; Zhao, X.; Gao, J.; Jing, W.; Zhang, X.; Li, J.; Li, Y.; Yang, J.; Liu, W. An Ultrasoft Self-Fused Supramolecular Polymer Hydrogel for Completely Preventing Postoperative Tissue Adhesion. *Adv. Mater.* **2021**, *33*, 2008395.
28. Min, J.; Zhou, Z.; Wang, H.; Chen, Q.; Hong, M.; Fu, H. Room Temperature Self-Healing and Recyclable Conductive Composites for Flexible Electronic Devices Based on Imine Reversible Covalent Bond. *Journal of Alloys and Compounds* **2022**, *894*, 162433.

Publisher's Note The Polymer Society of Korea remains neutral with regard to jurisdictional claims in published articles and institutional affiliations.